Received December 5, 2021, accepted January 6, 2022, date of publication January 12, 2022, date of current version January 18, 2022.
Digital Object Identifier 10.1109/ACCESS.2022.3142506

Optimization of Power Dispatch With Load Scheduling for Domestic Fuel Cell-Based Combined Heat and Power System

LEEHTER YAO, (Senior Member, IEEE), AND J. C. TEO
Department of Electrical Engineering, National Taipei University of Technology, Taipei 10608, Taiwan
Corresponding author: Leehter Yao (ltyao@ntut.edu.tw)

This work was supported in part by the Ministry of Science and Technology, Taiwan, under Grant MOST 107-2221-E-027-086-MY3.

ABSTRACT This study proposes an optimization scheme of thermal power and electric power dispatch integrated with load scheduling for the domestic fuel cell-based combined heat and power (DFCCHP) system. The scheme is implemented in home energy management systems installed in smart homes. To provide accurate energy cost evaluation for the optimization scheme, the nonlinear electric efficiency characteristics of the fuel cell are approximated with a polynomial expression. Along with the inclusion of thermal power dispatch in the scheme, the nonlinear relationship between the thermal power and the electric power of the fuel cell is incorporated to design temperature constraints in the DFCCHP system. On top of the nonlinearity and complexity of the fuel cell, residential electric load scheduling and other energy sources including the power grid, PV panels, and battery energy storage are considered to ensure that the scheme takes a comprehensive energy management approach. Because of the nonlinearity that exists in the modeling of the DFCCHP system, a mixed-integer nonlinear programming formulation is utilized to solve the optimization problem. The scheme is tested in a day-ahead environment with time-varying electricity prices and natural gas prices. The optimization aims to minimize the electricity cost and natural gas cost. It is shown in the simulation that optimization scheme dispatches the electric power and thermal power in an optimal way so that the energy cost due to time-varying electricity prices and natural gas prices is minimized. The electricity cost optimization puts both power purchase and power selling into consideration. It is also shown in the simulation that the household loads are scheduled in an optimal way to the time slots with lower electricity prices in accordance with the optimal thermal and electric power dispatch.

INDEX TERMS Home energy management system, nonlinear optimization, combined heat and power, load scheduling, power dispatch, fuel cell, PV panels.

I. INTRODUCTION

Global electricity consumption has increased dramatically as the population grows and through technological and economic advances [1]. Burning fossil fuels, the most common way to generate electricity, accounts for the largest share of global electricity generation [2]. Conventional means of electricity generation have resulted in massive greenhouse gas emissions that have caused global warming issues. The environmental damage caused by global warming has prompted a shift toward reducing carbon emissions [3].

Fuel cells are regarded as a promising technique for future electricity generation because of their ability to efficiently produce clean electricity with low pollutant emissions and low noise levels [4]–[6]. While producing electricity, fuel cells also produce residual heat as a byproduct. If this residual thermal power is utilized, the energy efficiency of fuel cells can be further improved. This prompted the idea of using a fuel cell as a combined heat and power (CHP) system in residential houses to simultaneously provide electric and thermal power.

ENE-FARM in Japan and Lolland Hydrogen Community in Denmark are typical examples of current domestic fuel cell-based CHP systems [7]–[9]. In the near future, domestic fuel cell-based CHP (DFCCHP) systems are likely to become a common way to generate power due to the environmental issues related to carbon emissions [10]. The benefit of using DFCCHP systems will be greatly enhanced

The associate editor coordinating the review of this manuscript and approving it for publication was Pierluigi Siano.

if both electric and thermal power are integrated well and dispatched optimally. For this purpose, home energy management systems (HEMS) can be deployed in smart homes. HEMS refer to technological platforms installed in smart homes that comprise hardware and software with the overall functionality required for smart home energy management (i.e., monitoring the energy sources and home appliances). A thermal power and electric power dispatch scheme for DFCCHP systems can be formulated in HEMS according to household energy demands, energy prices, and any other related factors.

A thermal power and electric power dispatch optimization scheme for DFCCHP systems is primarily intended to minimize energy cost of DFCCHP systems. Hence, an accurate modeling of the natural gas consumption for the fuel cell is vital in formulating a thermal power and electric power dispatch scheme for DFCCHP systems. This requires knowledge of the electric efficiency of fuel cells. In reality, the electric efficiency of a fuel cell varies nonlinearly with its generated electric power [11], [12]. This nonlinearity causes considerable complexity in the power dispatch scheme for DFCCHP systems. To avoid this complexity, some articles have formulated power dispatch schemes for DFCCHP systems by assuming that the electric efficiency of a fuel cell is constant [13]–[17]. However, this approach does not result in an accurate energy cost evaluation of the power dispatch scheme. To put it in perspective, suppose that a given fuel cell has an electric efficiency of 50% when it delivers 2.5 kW of electric power and 30% when it delivers 5 kW [18]. In this case, the fuel cell consumes 5 kW worth of natural gas if it delivers 2.5 kW of electric power (calculated by 2.5 kW/0.5). If the fuel cell delivers 5 kW of electric power, it consumes nearly 3.5 times as much natural gas as when it delivers 2.5 kW of electric power (calculated by 5 kW/0.3 = 16.67 kW). Consequently, if a constant is used to represent the electric efficiency of fuel cells, it would result in a less accurate energy cost evaluation for the power dispatch scheme of the DFCCHP system. Typically, power dispatch schemes for any types of power system search for optimal power dispatch according to the energy cost function values calculated by their cost functions [19]–[21]. By using a less accurate energy cost evaluation to formulate the cost function for calculating energy cost corresponding to any power dispatch decision, the formulated cost function will be not so accurate and might mislead the power dispatch scheme to make a less appropriate power dispatch decision. Therefore, the nonlinear variation of the electric efficiency for the fuel cell must be considered in order to develop an appropriate power dispatch scheme for DFCCHP systems.

In order to develop an appropriate power dispatch scheme for DFCCHP systems, several literatures incorporated the nonlinear variation of the electric efficiency for the fuel cell [22]–[26]. In [22], an analytical rule-based power dispatch strategy was proposed to optimize the power dispatch results according to the time-of-use prices as well as with electric and thermal demands considering the nonlinear variation of the electric efficiency for the fuel cell. In [23], an electric power and thermal power dispatch optimization scheme was presented to optimize the electric and thermal power dispatch of a DFCCHP system considering the nonlinear variation of the electric efficiency for the fuel cell. A similar optimization scheme was also presented in [24]. In [25], the Real Coded Genetic Algorithm is utilized to determine the optimal electric and thermal power dispatch of a DFCCHP system considering the nonlinear variation of the electric efficiency for the fuel cell. In [26], the Colonial Competitive Algorithm was utilized to determine the optimal electric and thermal power dispatch for a DFCCHP system considering the nonlinear variation of the electric efficiency for the fuel cell. Although it is rarely seen, [27] proposed a power dispatch scheme that incorporated thermal load scheduling. However, the scheme proposed in [27] was formulated for dispatching a fossil fuel-based CHP system rather than a DFCCHP system.

This paper proposes a comprehensive energy management scheme for DFCCHP systems while incorporating optimal residential electric load scheduling. Besides the electric power generated from the fuel cell, the proposed scheme optimizes the power from the PV panels, the batteries, and the power grid, making it a comprehensive energy management scheme for DFCCHP systems. The proposed scheme also minimizes the energy cost due to the natural gas consumption and energy purchased from or sold to the power grid. Additionally, it optimizes the scheduling of residential appliances. Although there is some research available that investigates residential load scheduling schemes, only a minimal amount explores the feasibility of integrating electric load scheduling with the electric and thermal power dispatch schemes for DFCCHP systems. To realize a more realistic residential environment, the residential electric loads are categorized into three types in the proposed scheme: interruptible, uninterruptible, and time-varying appliance loads.

The proposed power dispatch scheme involves mixed integers, nonlinear objective functions, and nonlinear constraints, making the entire scheme a mixed-integer nonlinear programming (MINLP) formulation. The MINLP problem can be solved using deterministic algorithms such as generalized bender decomposition, nonlinear branch and bound, and outer approximation [28]–[30]. Note that some research has applied heuristic algorithms such as particle swarm optimization, differential evolution, and genetic algorithms to solve MINLP problems [31]–[33]. However, this paper's proposed MINLP formulation is solved using a nonlinear branch and bound algorithm.

The fuel cell described in this paper uses natural gas through a reformer as the fuel [34]. The auxiliary burner also uses natural gas as a direct fuel. For this reason, the energy cost of the DFCCHP system is highly dependent on natural gas prices. The time-of-use models for natural gas were utilized in [35] and [36]. This paper investigates the effectiveness of the proposed power dispatch scheme in dealing with time-varying natural gas prices. Note that all the previously published power dispatch schemes for DFCCHP systems have not been tested in a time-varying natural gas price environment.

The major novelties and contributions of this paper are summarized as follows.

1) A comprehensive power dispatch scheme is proposed to minimize the energy cost for DFCCHP systems. The residential energy resources are optimized using the HEMS including the power from the fuel cell, the PV panels, the batteries, and the power purchased or sold to the grid.
2) To make the proposed scheme a more comprehensive energy management scheme for DFCCHP systems, residential electric load scheduling is considered in the proposed scheme. To realize a more realistic residential environment, the electric loads are categorized into interruptible, uninterruptible and time-varying appliances.
3) An optimization based on MINLP is proposed to solve the nonlinear optimization problem that involves electric and thermal power dispatch and electric load scheduling.
4) The proposed optimal power dispatch is conducted under the environment of time-varying natural gas prices and electricity prices.

The rest of this paper is organized as follows: Section II introduces the problem statement and the HEMS for the DFCCHP system. Section III describes the residential electric loads considered in this work as well as their constraints. Section IV describes the battery energy storage and hot water storage considered in this work and their constraints. Section V explains the fuel cell and the power grid considered in this work and their constraints. Section VI investigates the nonlinear variation of the fuel cell's electric efficiency and the nonlinear relationship between thermal power and electric power. Section VII presents the objective function of the proposed optimization model. Section VIII presents the simulation results and the discussion. Finally, section IX concludes.

II. HOME ENERGY MANAGEMENT SYSTEM FOR DOMESTIC FUEL CELL-BASED COMBINED HEAT AND POWER SYSTEMS

This paper proposes an optimal thermal power and electric power dispatch scheme integrated with optimal residential load scheduling for a DFCCHP system. To enable accurate energy cost evaluation, the proposed scheme is formulated by considering the nonlinear variation of the fuel cell's electric efficiency. Figure 1 depicts the residential energy system considered in formulating the proposed energy dispatch. This energy system comprises various types of energy sources including the PV panels, the battery, the fuel cell, and the power grid.

As the core of the DFCCHP system, the fuel cell simultaneously provides electric and thermal energy using natural gas as its fuel, meaning that the fuel cell is equipped with a reformer that extracts pure hydrogen from natural gas and provides it to the fuel cell. The auxiliary burner produces thermal energy by also using natural gas. The hot water storage is used to store the hot water. All the required domestic hot water is from the hot water storage. The volume of the hot water in the hot water storage remains constant all time, i.e., when a particular amount of water is consumed from the hot water storage, the same amount of cold water is refilled into the hot water storage. The thermal power generated from the residual heat of the fuel cell and the auxiliary burner are used to heat the hot water in storage. Therefore, the thermal energy resources in the DFCCHP system include the fuel cell and the auxiliary burner.

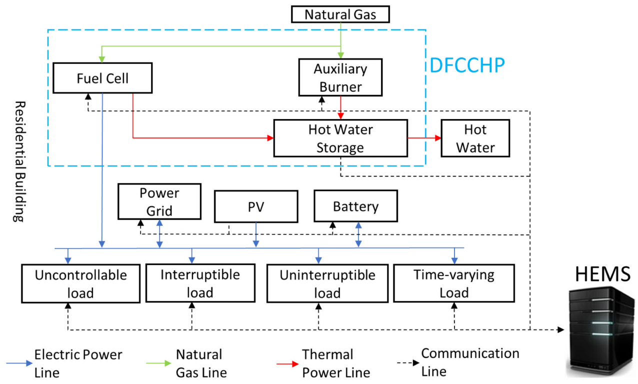

FIGURE 1. The residential energy system considered in this work.

The electric energy resources in the DFCCHP system include the power grid, PV panels, battery and the fuel cell. The electric load can be divided into controllable and uncontrollable loads. The controllable loads are the loads that can be scheduled to the time slots with lower energy prices whereas the uncontrollable loads do not provide this flexibility. The controllable loads are further categorized into interruptible, uninterruptible, and time-varying loads. The interruptible loads can be interrupted at any time; the uninterruptible loads, once started, must operate continuously for a certain period of time without interruption to properly complete the tasks. Like uninterruptible loads, once started, time-varying loads cannot be interrupted until they have completed their task.

Electric power can be purchased or sold to the power grid. A HEMS is implemented with a computer that controls and monitors the energy resources and appliances in the residential energy system through home area networks. The time-varying electricity and natural gas prices are adopted. The cost of electricity and natural gas consumed by the DFCCHP system are calculated based on the time-varying electricity and natural gas prices, respectively. Electricity is sold back to the grid based on the same time-varying electricity prices. An optimal power dispatch scheme is proposed and implemented in HEMS so that the minimum energy cost is attained by optimally dispatching both electric and thermal power. An optimal scheduling scheme for those three types of schedulable loads is also designed along with the proposed optimal power dispatch. The MINLP is utilized for energy cost minimization according to the time-varying electricity prices and natural gas prices.

III. HOUSEHOLD ELECTRIC LOADS

Within three types of controllable loads, let A_{c1}, A_{c2} and A_{c3} be the sets of interruptible, uninterruptible and time-varying loads, respectively. Denote the set of uncontrollable loads as A_{uc}. The sampling interval is denoted as T_s minutes, and it is assumed that the entire scheduling horizon for the HEMS to perform scheduling is 1 day (i.e., 24 h). There are N sampling intervals in the entire scheduling horizon, where $N = 1440/T_s$.

Let $r_a^j \in \{0, 1\}$ be the on/off status of the a-th appliance such that $r_a^j = 0$ indicates that the appliance is turned off at the j-th sampling interval and $r_a^j = 1$ indicates the opposite, $j = 0, \ldots N-1, \forall a \in (A_{c1} \cup A_{c2} \cup A_{c3})$. Every a-th appliance can be pre-assigned with an allowable operation interval denoted by τ_a^s and τ_a^e, where $\tau_a^s, \tau_a^e \in [0, N-1]$. The HEMS can control the on/off status of a-th appliance only during the operation interval $\left[\tau_a^s, \tau_a^e\right]$. If it is not in the permitted time range, $r_a^j = 0$. Hence,

$$r_a^j = \begin{cases} \beta, \beta \in \{0, 1\}, & j \in \left[\tau_a^s, \tau_a^e\right], \\ 0, & \text{otherwise}; \end{cases} \quad \forall a \in (A_{c1} \cup A_{c2} \cup A_{c3}). \tag{1}$$

The power consumption of each interruptible appliance is assumed to be constant. Denote the rated power of the a-th interruptible appliance as $P_a^{\max}$,

$$P_a^j = \begin{cases} r_a^j P_a^{\max}, & j \in \left[\tau_a^s, \tau_a^e\right], \\ 0, & \text{otherwise}; \end{cases} \quad \forall a \in A_{c1}. \tag{2}$$

Although the interruptible appliances can be interrupted at any time, the work performed by interruptible appliances should be regulated such that they operate for at least a certain number of sampling intervals to avoid affecting the comfort of the dwelling members too much. For example, although a water pumping motor can be interrupted by the HEMS at any time, it should be regulated to pump water for at least a certain number of sampling intervals each day so that there is enough water stored for use.

For every a-th appliance belonging to the set of interruptible loads A_{c1}, assume that they must operate for at least Q_a sampling intervals every day, i.e.,

$$\sum_{j=\tau_a^s}^{\tau_a^e} r_a^j \geq Q_a, \quad \forall a \in A_{c1}. \tag{3}$$

For uninterruptible and time-varying appliances, HEMS determines a starting time within their operation interval. Once these appliances have started, they cannot be interrupted before they completed their task.

Assume that the a-th uninterruptible and time-varying appliances, after started, must operate continuously for Γ_a sampling intervals. For the optimization scheme implemented in the HEMS to find the optimal starting time for the uninterruptible and time-varying appliances, an auxiliary binary variable $\delta_a^j \in \{0, 1\}, \forall a \in (A_{c2} \cup A_{c3})$, is introduced. Note that $\delta_a^j = 1$ indicates that the a-th uninterruptible or time-varying appliance is started at the j-th sampling interval and that $\delta_a^j = 0$ indicates the opposite. Once δ_a^j is set to 1 at the j-th sampling interval, then from the j-th sampling interval onwards, $r_a^j = 1$ consecutively for Γ_a sampling intervals without interruption. The constraints for the optimization can set as:

$$\sum_{j=\tau_a^s}^{\tau_a^e - \Gamma_a + 1} \delta_a^j = 1, \tag{4}$$

$$r_a^{j+n} \geq \delta_a^j, n = 0, \ldots, (\Gamma_a - 1), \quad \forall a \in (A_{c2} \cup A_{c3}). \tag{5}$$

The power consumption of uninterruptible appliances is constant, whose definition is similar to (2). Thus,

$$P_a^j = \begin{cases} r_a^j P_a^{\max}, & j \in \left[\tau_a^s, \tau_a^e\right]; \\ 0, & \text{otherwise}; \end{cases} \quad \forall a \in A_{c2}. \tag{6}$$

As for the time-varying appliances, assume that once they have started, their time-varying load at each sampling interval is $\sigma_a^n, n = 0, \ldots, (\Gamma_a - 1)$; then the power consumption of time-varying appliances can be defined as:

$$P_a^{j+n} = \begin{cases} r_a^{j+n} \sigma_a^n, & n = 0, \ldots, (\Gamma_a - 1); \\ 0, & \text{otherwise}; \end{cases} \quad \forall a \in A_{c3}. \tag{7}$$

If P_L^j is denoted as the total residential load at the j-th sampling interval, then

$$P_L^j = \sum_{a \in A_{c1} \cup A_{c2} \cup A_{c3} \cup A_{uc}} P_a^j. \tag{8}$$

IV. BATTERY AND HOT HOTWATER STORAGE

It is assumed that the battery is only allowed to work in one state (either charge or discharge) at each sampling interval. To realize this statement, the following constraint is applied:

$$\mu_{ch}^j + \mu_{dch}^j \leq 1, \tag{9}$$

where $\mu_{ch}^j, \mu_{dch}^j \in \{0, 1\}$ are the binary variables indicating the charging statuses of the battery. $\mu_{ch}^j = 1$ or $\mu_{dch}^j = 1$ indicate the battery is charging or discharging at the j-th sampling interval; $\mu_{ch}^j = 0$ or $\mu_{dch}^j = 0$ indicate the battery is not charging or discharging.

To prevent battery damage, it is necessary to ensure that the battery charging and discharging power (P_{ch}^j and P_{dch}^j, respectively) is kept within a given range bounded by lower and upper bounds $P_{dch}^{\min}$ and $P_{dch}^{\max}$ for discharging, $P_{ch}^{\min}$ and $P_{ch}^{\max}$ for charging. Therefore,

$$P_{ch}^{\min} \leq \frac{P_{ch}^j}{\eta_{ch}} \leq \mu_{ch}^j P_{ch}^{\max}; \tag{10}$$

$$P_{dch}^{\min} \leq P_{dch}^{j}\eta_{dch} \leq \mu_{dch}^{j}P_{dch}^{\max}; \tag{11}$$

where η_{ch} and η_{dch} represent the charging and discharging efficiencies of the battery where $\eta_{ch}, \eta_{dch} \leq 1$.

To prevent the battery from being overcharged or over discharged, the state of charge (SOC) of the battery at every j-th sampling interval is also constrained by lower and upper bounds (SOC^{min} and SOC^{max}, respectively), i.e.,

$$SOC^{\min} \leq SOC^{j} \leq SOC^{\max}. \tag{12}$$

The SOC of the battery at every j-th sampling intervals is modeled as follows:

$$SOC^{j} = SOC^{j-1} + \frac{P_{ch}^{j} - P_{dch}^{j}}{E_{batt}}T_{s}, \tag{13}$$

where E_{batt} is the full capacity of the battery.

If P_{batt}^{j} is denoted as the power of battery at the j-th sampling interval, then

$$P_{batt}^{j} = \frac{P_{ch}^{j}}{\eta_{ch}} - P_{dch}^{j}\eta_{dch}. \tag{14}$$

P_{batt}^{j} is positive if the battery is charging and negative if the battery is discharging.

Denote V_{total} as the total volume of water in the hot water storage, V_{total} is assumed to remain constant at all time. Thus, when a certain amount of hot water is consumed, the same amount of cold water is allowed to flow into the water storage to replace the consumed hot water. For the convenience of analysis, no thermal loss is assumed in the hot water storage. When a particular volume of cold water enters the hot water storage at the j-th sampling interval, the temperature of the cold water will be raised to the temperature of the water in storage before the cold water entered (at the (j-1)-th sampling interval). Denote V_{cold}^{j} and T_{cold}^{j} as the volume and temperature of the cold water entering the hot water storage at the j-th sampling interval, respectively. Let T_{st}^{j} represent the temperature of the hot water storage at the j-th sampling interval. If some hot water is consumed at the j-th sampling interval, then an equivalent volume V_{cold}^{j} of cold water with temperature T_{cold}^{j} is refilled to maintain the constant total volume V_{total} of the hot water storage. The additional thermal energy that the thermal resources require to compensate for this is calculated as $V_{cold}^{j}\left(T_{st}^{j-1} - T_{cold}^{j}\right)C_{water}$. The thermal energy required to raise the hot water storage temperature from T_{st}^{j-1} to T_{st}^{j} is calculated as $V_{total}\left(T_{st}^{j} - T_{st}^{j-1}\right)C_{water}$, where C_{water} is the specific heat of water.

The hot water storage is heated by the thermal power from the fuel cell's residual heat and from direct heating by the auxiliary burner. The thermal energy supplied to the hot water storage at the j-th sampling interval can be calculated as $\left(H_{FC}^{j} + H_{aux}^{j}\right)T_{s}$, where H_{FC}^{j} and H_{aux}^{j} are the residual thermal power of the fuel cell and the thermal power from the auxiliary burner at the j-th sampling interval, respectively. With the above-mentioned statements, the thermal energy balance of the hot water storage between two consecutive sampling intervals can be defined as:

$$V_{cold}^{j}\left(T_{st}^{j-1} - T_{cold}^{j}\right)C_{water} + V_{total}\left(T_{st}^{j} - T_{st}^{j-1}\right)C_{water} = \left(H_{FC}^{j} + H_{aux}^{j}\right)T_{s}. \tag{15}$$

By rearranging (15), the hot water temperature at the j-th sampling interval can be modeled as:

$$T_{st}^{j} = \frac{V_{cold}^{j}\left(T_{cold}^{j} - T_{st}^{j-1}\right) + V_{total}T_{st}^{j-1}}{V_{total}} + \frac{H_{FC}^{j} + H_{aux}^{j}}{V_{total}C_{water}}T_{s}. \tag{16}$$

To prevent the hot water storage temperature from being too hot or too cold, the temperature of the hot water storage at any j-th sampling interval is constrained by the lower and upper bounds $T_{st}^{\min}$ and $T_{st}^{\max}$, respectively. Thus,

$$T_{st}^{\min} \leq T_{st}^{j} \leq T_{st}^{\max}. \tag{17}$$

V. FUEL CELL AND POWER GRID

The electric power of the fuel cell P_{FC}^{j} at any j-th sampling interval must be constrained by lower and upper bounds to prevent it from underloading or overloading. Hence, the following constraint is applied:

$$P_{FC}^{\min} \leq P_{FC}^{j} \leq P_{FC}^{\max}, \tag{18}$$

where $P_{FC}^{\min}$ and $P_{FC}^{\max}$ denote the lower and upper bounds, respectively, for fuel cell's generated power. To prevent the fuel cell from charging or discharging too fast, the rate of change in fuel cell's electric output must also be constrained by an upper and lower limit (ΔP_{FC}^{U} and ΔP_{FC}^{L}) as follows:

$$P_{FC}^{j} - P_{FC}^{j-1} \leq \Delta P_{FC}^{U}, \tag{19}$$

$$P_{FC}^{j-1} - P_{FC}^{j} \leq \Delta P_{FC}^{L}. \tag{20}$$

Denote P_{grid}^{j} as the power purchased or sold to the power grid at the j-th sampling interval. It also needs to be constrained by an upper and lower limit ($P_{grid}^{\max}$ and $P_{grid}^{\min}$) as follows:

$$P_{grid}^{\min} \leq P_{grid}^{j} \leq P_{grid}^{\max}, \tag{21}$$

where P_{grid}^{j} is positive if electric power is purchased from the power grid and negative P_{grid}^{j} if it is sold to the power grid.

Let P_{PV}^{j} be the power generated from PV panels at the j-th sampling interval. The electric power in the DFCCHP system remains balanced as follows:

$$P_{grid}^{j} + P_{PV}^{j} + P_{FC}^{j} - P_{batt}^{j} = P_{L}^{j}. \tag{22}$$

VI. ELECTRIC AND THERMAL EFFICIENCIES OF FUEL CELLS

The electric efficiency η_{FC}^{j} of the fuel cell at the j-th sampling interval is defined as the ratio of generated electric power P_{FC}^{j} to the consuming rate of natural gas φ_{FC}^{j}, i.e.,

$$\eta_{FC}^{j} = P_{FC}^{j}/\varphi_{FC}^{j}. \tag{23}$$

The electric efficiency η_{FC}^j is essentially a nonlinear function of the generated electric power. Denote ζ^j as the part load ratio (*PLR*) of the fuel cell at the *j*-th sampling interval, i.e. $\zeta^j = P_{FC}^j / P_{FC}^{\max}$, a fifth-order polynomial of ζ^j is utilized to approximate the nonlinear relationship between η_{FC}^j and P_{FC}^j as follows:

$$\eta_{FC}^j = a_1 \left(\zeta^j\right)^5 + a_2 \left(\zeta^j\right)^4 + a_3 \left(\zeta^j\right)^3 + a_4 \left(\zeta^j\right)^2 + a_5 \zeta^j + a_6, \quad (24)$$

where $a_1 \ldots a_6$ are the polynomial coefficients.

This paper adopts the fuel cell presented in [23]. Using curve fitting to construct a mathematical function describing the relationship between the electric efficiency and *PLR* of the fuel cell, it is obtained that $a_1 = 0.9033$, $a_2 = -2.9996$, $a_3 = 3.6503$, $a_4 = -2.0704$, $a_5 = 0.4623$ and $a_6 = 0.3747$. Notably, these values are obtained by considering that the fuel cell only operates within the operating region of $PLR \geq 0.05$. Different coefficients will be obtained when referring to different fuel cells with different operating conditions. The HEMS is designed to minimize the energy cost (including the cost of electricity and natural gas). As the optimization scheme searches for the optimal generated power P_{FC}^j of the fuel cell in the DFCCHP system, the consuming rate φ_{FC}^j of natural gas to generate the required generated power is calculated on the basis of (23) with the nonlinear electric power efficiency η_{FC}^j given in (24). In other words,

$$\varphi_{FC}^j = P_{FC}^j / (a_1 \left(\zeta^j\right)^5 + a_2 \left(\zeta^j\right)^4 + a_3 \left(\zeta^j\right)^3 + a_4 \left(\zeta^j\right)^2 + a_5 \zeta^j + a_6). \quad (25)$$

It is shown in (25) that the natural gas consumption rate is a nonlinear function of P_{FC}^j.

The byproduct of a fuel cell's generated electric power is the residual heat. The thermal efficiency r_{FC}^j is defined as the ratio of the thermal power H_{FC}^j to the fuel cell's generated power P_{FC}^j, calculated as follows:

$$r_{FC}^j = H_{FC}^j / P_{FC}^j. \quad (26)$$

The thermal efficiency r_{FC}^j is also a nonlinear function of the generated electric power P_{FC}^j. A fourth-order polynomial of PLR ζ^j is utilized to approximate the nonlinear relationship between r_{FC}^j and P_{FC}^j as follows:

$$r_{FC}^j = b_1 \left(\zeta^j\right)^4 + b_2 \left(\zeta^j\right)^3 + b_3 \left(\zeta^j\right)^2 + b_4 \zeta^j + b_5, \quad (27)$$

where $b_1 \ldots b_5$ are the coefficients of the polynomial in (27). The residual heat of the fuel cell is utilized as part of the thermal energy resources of the hot water storage. The residual thermal power H_{FC}^j of the fuel cell is proportional to the generated power P_{FC}^j, i.e.,

$$H_{FC}^j = P_{FC}^j (b_1 \left(\zeta^j\right)^4 + b_2 \left(\zeta^j\right)^3 + b_3 \left(\zeta^j\right)^2 + b_4 \zeta^j + b_5). \quad (28)$$

Using curve fitting to construct a mathematical function describing the relationship between the r_{FC}^j and *PLR* of the fuel cell, the following is obtained: $b_1 = 1.0785$, $b_2 = -1.9739$, $b_3 = 1.5005$, $b_4 = -0.2817$ and $b_5 = 0.6838$.

If the thermal power of the residual heat is not enough to heat the water in the hot water storage so that the constraint for the hot water temperature T_{st}^j in (17) is satisfied, the auxiliary burner is designed to provide the additional thermal power. The auxiliary burner's thermal power at the *j*-th sampling interval is denoted as H_{aux}^j. An optimal H_{aux}^j will be searched for according to the constraints satisfying the thermal balance equation in (15) and (17). Recall that the auxiliary burner also uses natural gas as the fuel. Denote φ_{aux}^j as the natural gas consuming rate for the auxiliary burner, η_{aux} as the efficiency of the auxiliary burner. The burner is a regular heating facility that heats inlet cold water to a preset temperature satisfying the constraint in (17) by directly burning natural gas. Different from the fuel cell efficiency in (24), the auxiliary burner's efficiency η_{aux} is a constant because no chemical reaction is involved in the heating process. There is a constant relationship between the natural gas consuming rate φ_{aux}^j and the generated thermal power H_{aux}^j for the auxiliary burner as follows:

$$\varphi_{aux}^j = H_{aux}^j / \eta_{aux} \quad (29)$$

where η_{aux} is a constant.

VII. OBJECTIVE FUNCTION

The objective function for the nonlinear optimization in the HEMS is to minimize the energy cost that is divided into two parts (including the electricity cost and natural gas cost). The day-ahead electricity prices and natural gas prices are assumed in this paper. If ρ^j and υ^j are the electricity price and natural gas price at the *j*-th sampling interval, respectively, the objective function for the optimization can be defined as follows:

$$\min_{\substack{r_a^j, j=k,\ldots,N-1, a\in A_{c1}\cup A_{c2}\cup A_{c3} \\ \delta_a^j, j=k,\ldots,N-1, a\in A_{c2}\cup A_{c3} \\ P_{grid}^j, j=k,\ldots,N-1 \\ P_{ch}^j, j=k,\ldots,N-1 \\ P_{dch}^j, j=k,\ldots,N-1 \\ \mu_{ch}^j, j=k,\ldots,N-1 \\ \mu_{dch}^j, j=k,\ldots,N-1 \\ P_{FC}^j, j=k,\ldots,N-1 \\ H_{aux}^j, j=k,\ldots,N-1}} \sum_{j=k}^{N-1} \rho^j P_{grid}^j T_s + \upsilon^j \varphi_{FC}^j T_s + \upsilon^j \varphi_{aux}^j T_s$$
$$\text{subject to (3),(4),(5),(9),(10),(11),(12),(17),(18),(19),(20),(21),(22).} \quad (30)$$

Note that the proposed optimization in (30) is a real-time optimization scheme. Both the thermal power and electric power dispatch, as well as the load scheduling are planned from the current *k*-th sampling interval to the end of day (the *N*-th sampling interval). The same optimization scheme is conducted iteratively as time goes to the next sampling interval, and so on.

The objective function to be minimized in (30) is the total cost of energy including the electricity cost in the first term, the fuel cell's natural gas cost in the second term, and the auxiliary burner's natural gas cost in the third term. The constraints for the loads are formulated in (3)-(5) while the constraints for the battery are shown in (10)-(12). The hot water temperature is constrained within a range as in (17), the generated power from the fuel cell is constrained as in (18)-(20). Finally, the grid power is constrained in (21), the power balance equation as in (22) is also a constraint.

The optimization in (30) is a mixed-integer problem because the optimization variables consists of both binary and real variables. Additionally, the objective function and some constraints are nonlinear. The optimization in (30) is formulated as a MINLP problem.

VIII. SIMULATION RESULTS AND DISCUSSION

To perform the simulation, the proposed scheme is first modeled in A Mathematical Programming Language (AMPL). The commercial nonlinear solver KNITRO is then used to solve the proposed scheme. KNITRO is a commercial solver that solves large-scale MINLP problems by using a nonlinear branch and bound algorithm [23]. It is widely used in business and other industries because of its efficiency and robustness. All the computer simulations are made on a personal computer with Intel Core i7-3770 CPU @ 3.8 GHz and 128 GB RAM.

A. SIMULATION SETTING

The entire scheduling horizon for the proposed scheme to perform power dispatch is 24 h. The proposed scheme performs power dispatch optimization at every sampling interval in the scheduling horizon. The sampling interval is set as $T_s = 15$minutes. Hence, 96 sampling intervals are in the entire scheduling horizon.

The electric power from the power grid at every sampling interval P^j_{grid} are bounded between $P^{\min}_{grid} = -1.5$kW and $P^{\max}_{grid} = 3.2$kW. The electric power from the fuel cell at every sampling interval P^j_{FC} are bounded between $P^{\min}_{FC} = 0.3$kW and $P^{\max}_{FC} = 5$kW. The lower and upper limits for battery charging power at every sampling interval are set as $P^{\min}_{ch} = 0$kW and $P^{\max}_{ch} = 1.53$kW, respectively. Similarly, the lower and upper limits for battery discharging power at every sampling interval are set as $P^{\min}_{dch} = 0$kW and $P^{\max}_{dch} = 1.53$kW, respectively. The SOC of the battery is bounded between $SOC^{\min} = 0.3$ and $SOC^{\max} = 0.9$. The initial SOC is set as 0.6. The battery capacity is set as $E_{batt} = 15.3$kWh. Of course, the battery capacity can also be reasonably reduced due to cost concern.

The hot water storage temperature at every sampling interval T^j_{st} are set to range between $T_{st,\min} = 60$°C and $T_{st,\max} = 80$°C. Since the temperature of cold water entering the hot water storage does not vary too much in a day, V^j_{cold} is

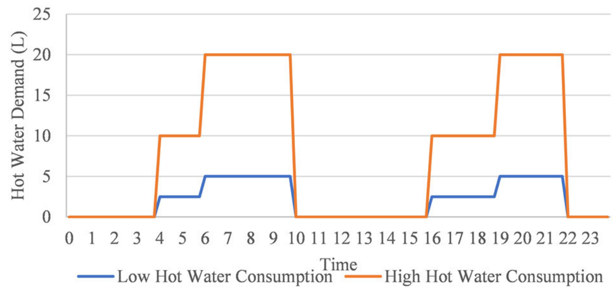

FIGURE 2. The expected hot water demand.

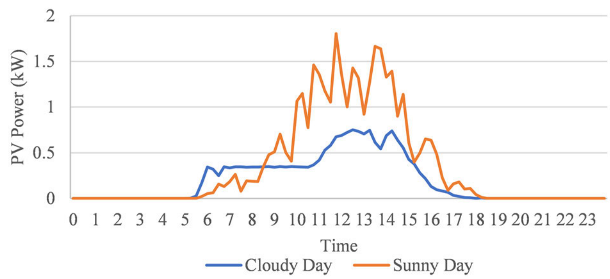

FIGURE 3. Forecasted solar energy generation profile from PV panels.

set as 20°C for the entire scheduling horizon. It is not unusual to assume that the cold water temperature remains constant throughout the entire scheduling horizon [37].

The total volume of the hot water storage, V_{total}, is set as 150 L. The efficiency of the auxiliary burner η_{aux} is set as 0.86 [37]. The specific heat of water is set as 0.001161 kWh/L·°C [38]. The expected hot water demands are shown in Figure 2. Two types of hot water demand profiles including high demand and low demand are defined in Figure 2 for simulation.

Figure 3 shows the day-ahead forecast of solar energy generation profiles from the PV panels for both sunny and cloudy days. Table 1 shows the parameters of electric loads including their allowed operating time range, rated power consumption, and the minimum operation duration requirement.

B. SIMULATION RESULTS

Four cases are simulated as illustrated in Table 2. Figures 4–7 illustrate the results of electric load scheduling for these four cases. Figures 8–11 show the thermal power dispatching results of the auxiliary burner for these four cases. Detailed explanations to these Figures are as follows.

Referring to Table 2, the simulation settings for cases 1 and 2 are the same except for the hot water demand profiles. Similar insights are obtained when comparing case 3 with case 4. The settings in cases 1 and 3 are the same except for the weather type that leads to different solar energy generation. By comparing case 1 with case 3, it is noted that high solar energy generation helps a great deal in reducing the energy cost of a residential house. This is because solar energy is used to meet the need of residential

TABLE 1. Paramters of electric loads.

Load	Operating Time Range	Rated Power (kW)	Required Operating Duration (Sampling Interval)
Uncontrollable Load	0:00-0:00	0.4	96
Interuptible Load 1	0:00-7:00, 19:00-23:45	0.4	4,6
Interuptible Load 2	7:00-10:00 14:00-17:00	0.4	2,5
Interuptible Load 3	12:00-15:00, 18:00-21:00	0.6	5,2
Uninteruptible Load 1	9:00-12:00	0.7	3
Uninteruptible Load 2	15:00-18:00	0.7	3
Uninteruptible Load 3	21:00-23:45	0.7	3
Variable Load 1	7:00-14:00	0.4,0.5,0.6	1,1,1

TABLE 2. Simulation results.

Case	Weather	Hot Water Demand Profile	Energy Cost (NTD)	Computational Time (Sec)
Case 1	Cloudy	Low	67.81	168.04
Case 2		High	191.29	240.03
Case 3	Sunny	Low	53.20	320.71
Case 4		High	176.88	413.12

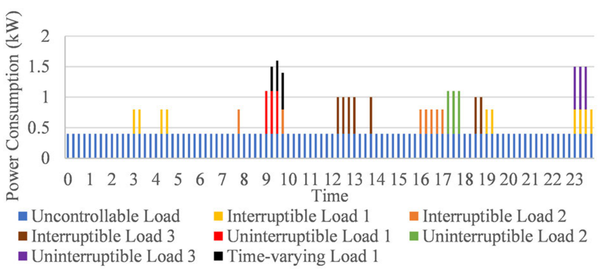

FIGURE 4. The results of electric load scheduling – case 1.

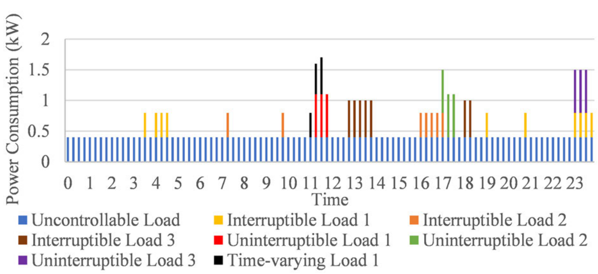

FIGURE 5. The results of electric load scheduling – case 2.

load when it is available, rather than purchasing power from the grid. Additionally, after the load is met, the DFCCHP system can sell the generated electric energy to the power grid

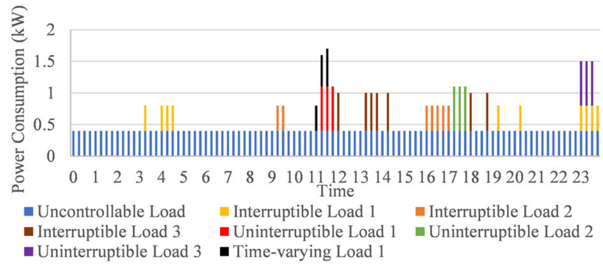

FIGURE 6. The results of electric load scheduling – case 3.

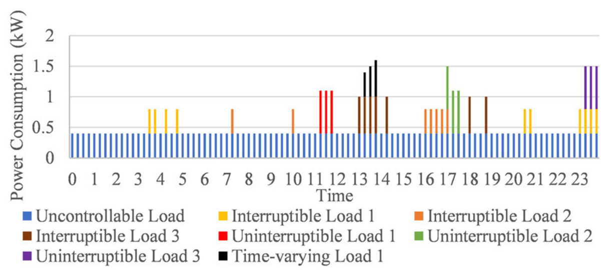

FIGURE 7. The results of electric load scheduling – case 4.

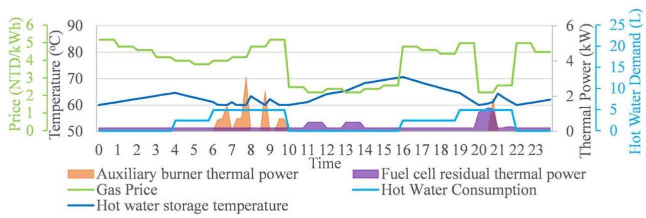

FIGURE 8. Dispatching results of the auxiliary burner – case 1.

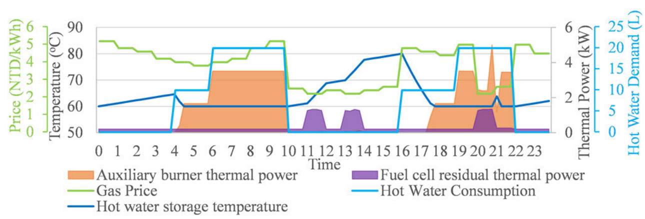

FIGURE 9. Dispatching results of the auxiliary burner - case 2.

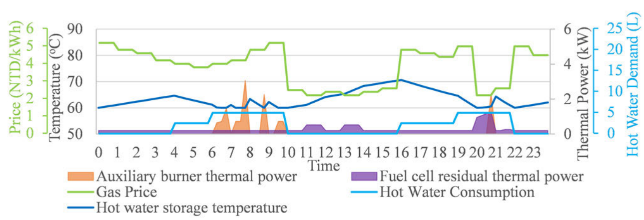

FIGURE 10. Dispatching results of the auxiliary burner - case 3.

to maximize profits, resulting in a lower total energy cost in case 3. Similar insights are obtained when comparing case 2 with case 4.

Although the optimal scheduling is conducted at every sampling interval, the computational time presented in

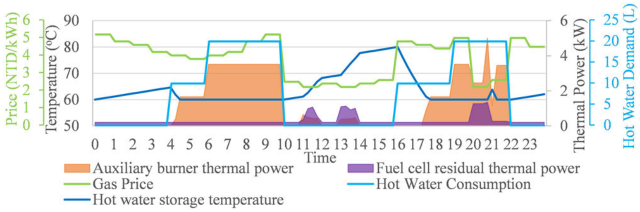

FIGURE 11. Dispatching results of the auxiliary burner - case 4.

Table 2 is the runtime of optimization conducted at the first sampling interval of the day, i.e., $k = 0$, for the convenience of comparison. It is seen that the computational time required to solve the proposed optimization scheme is relatively high in all cases due to the fact that the proposed scheme is an MINLP formulation. However, the runtimes for all cases are still much shorter than the sampling interval 15 minutes for the optimization. In other words, HEMS can still has enough time to run the optimization in (30) and control all loads responding to the scheduling results. When solving all the case studies at the subsequent sampling intervals of the day, a shorter scheduling horizon is considered and therefore the required runtime is also considerably reduced. Therefore, the average runtime required to solve the case studies at each sampling interval in the day will be much shorter than that presented in Table 2.

Referring to Figures 4–7, in all cases, all the electric loads are scheduled to operate within their respective allowable operating windows. Additionally, all the electric loads satisfy their respective constraints (implying that they are modeled correctly). For instance, the power consumption of time-varying load 1 in cases 1–4 does vary with operation cycle. The uninterruptible loads in cases 1–4 operate continuously for certain period of time without interruption once they are started. The interruptible loads can be discontinued and resumed within their respective allowed operation time range. All these observations indicate that all the electric loads are modeled correctly.

Figures 8–11 show the thermal energy optimal dispatching results of the auxiliary burner according to the residual thermal energy from the fuel cell and the variation of natural gas prices. By comparing cases 1 and 2, it is clear that the higher hot water demand in Figure 9 (compared with that in Figure 8) leads to higher thermal power dispatch from the auxiliary burner. Although the hot water demand occurs at the interval with higher natural gas prices, the thermal power dispatch of the auxiliary burner is optimized so that the burner is allowed to operate at the sampling intervals with natural gas prices are as low as possible. The same analysis applies to case 3 in Figure 10 and case 4 in Figure 11. Although the thermal power dispatch of the auxiliary burner corresponds with the hot water consumption profile, the auxiliary burner is not turned on as soon as the hot water consumption rises. The HEMS optimizes the auxiliary burner's thermal power dispatch so that the residual thermal energy from the fuel cell is fully utilized before the burner is turned on.

On sunny days, the fuel cell is not turned on as often as it is on cloudy days because there is more electricity generated from the PV panels on sunny days than on cloudy days. This results in less residual heat from the fuel cell on sunny days than cloudy days. Comparing Figures 9 and 11, it is observed that the auxiliary burner is turned on more often for case 4 in Figure 11 than for case 2 in Figure 9 despite the same thermal power demand profile. Figures 12–15 respectively show the electric power dispatch results from the grid, the fuel cell, and the battery at every sampling interval for cases 1–4. The dispatch results fulfilled all the imposed constraints in the DFCCHP system.

Referring to case 1 in Figure 12, it is obvious that the proposed scheme scheduled the electricity purchasing at the time when electricity prices were relatively low (e.g., 3:00 to 5:00 and 17:00 to 19:00). Conversely, electricity selling is scheduled at the time when electricity prices were relatively high (e.g., 10:00 to 16:00 and 20:00 to 23:00). Hence, the proposed optimization scheme achieves electricity cost savings by purchasing power from the grid at the sampling intervals with lower electricity prices and by selling it at the sampling intervals with higher electricity prices. When the natural gas prices are higher than the electricity prices, HEMS schedules the fuel cell to deliver less electric power. Conversely, when the natural gas prices are lower than the electricity prices, the HEMS allows the fuel cell to deliver more electricity. For example, the natural gas prices are higher than the electricity prices at 00:00-09:45, therefore the HEMS schedules the fuel cell to deliver minimum electric power. Same situations are observed at 16:00-19:45 and 22:00-23:45 where the proposed scheme scheduled the fuel cell to deliver minimum electric power due to the reason that the natural gas prices are higher than the electricity prices. At 10:00-16:00 and 20:00-22:00, the natural gas prices are lower than the electricity prices and therefore the HEMS allows the fuel cell to deliver more electric power at 11:00-12:00, 13:00-14:00 and 20:00-21:00. These observations indicate that the proposed optimization scheme achieves electricity cost savings by not only optimizing the electricity purchasing/selling, but also optimizing the fuel cell power dispatch.

Referring to the Case 2 in Figure 13, it is seen that most electricity purchasing is scheduled at the time when electricity prices are low, e.g., 3:00-5:00 and 17:00-19:00. Furthermore, most electricity selling is scheduled at the time when electricity prices are high, e.g., 10:00-16:00 and 20:00-23:00. The fuel cell is scheduled to deliver minimum power when natural gas prices are high, e.g., 00:00-09:45 and 16:00-19:45. The fuel cell is allowed to delivered higher electric power when natural gas prices are lower than the electricity prices, as evidenced by the cyan color humps at 11:00-12:00, 13:00-14:00, and 20:00-21:00. These again indicate that the proposed optimization scheme minimizes electricity cost by optimizing the electricity purchasing/selling and the fuel cell power dispatch. The insight obtained from analyzing Figure 12 and Figure 13 are

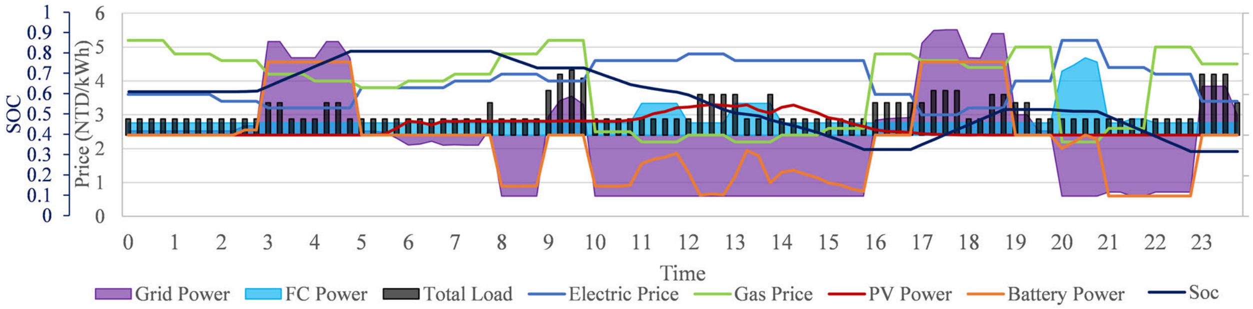

FIGURE 12. The power dispatch results for the energy sources - case 1.

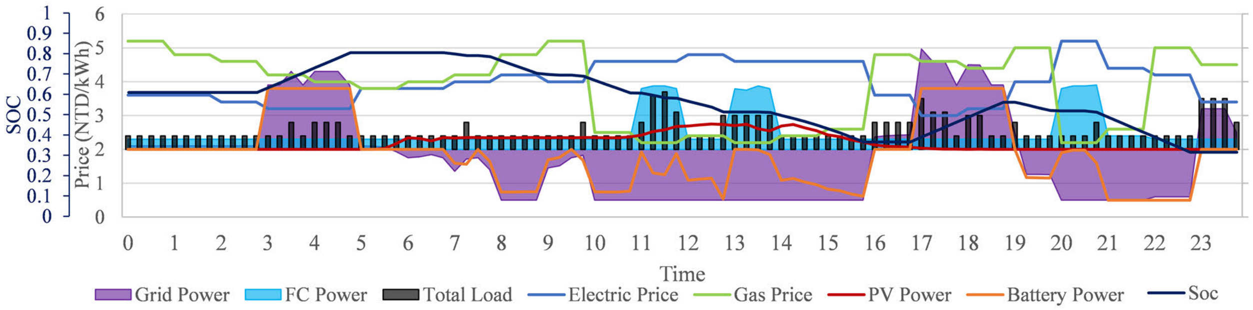

FIGURE 13. The power dispatch results for the energy sources - case 2.

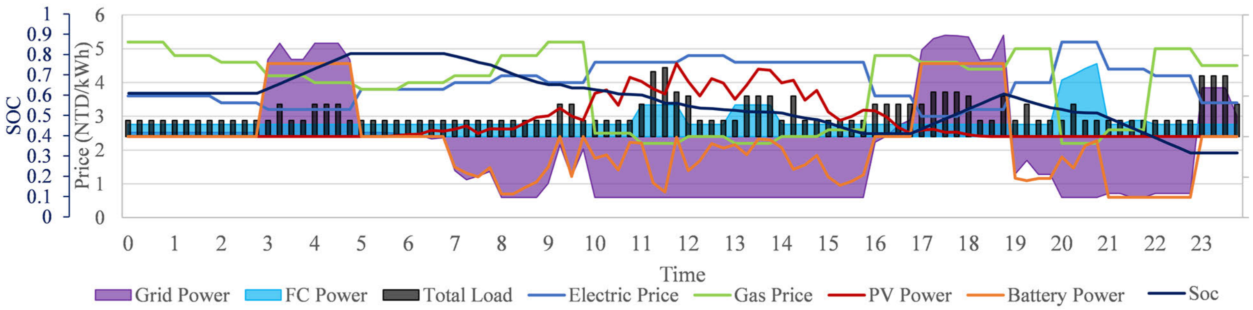

FIGURE 14. The power dispatch results for the energy sources - case 3.

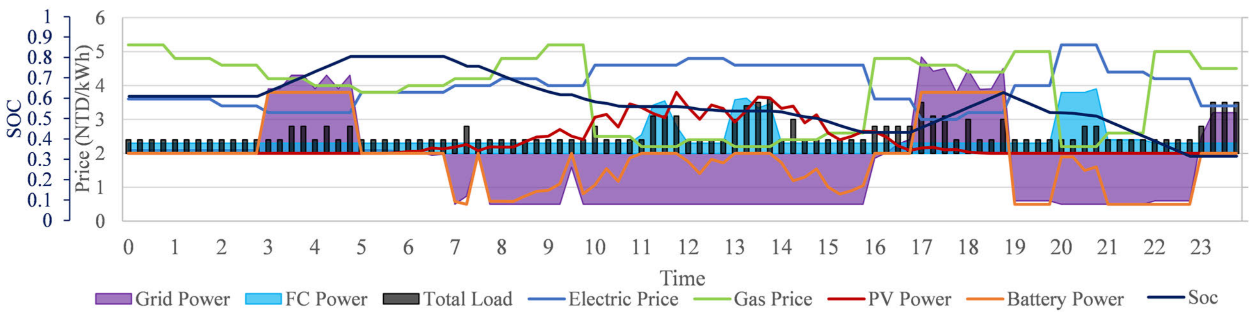

FIGURE 15. The power dispatch results for the energy sources - case 4.

also obtained in Figure 14 and 15. That is, the proposed scheme scheduled the electricity purchasing/selling at the time when electricity prices are low/high. The fuel cell is scheduled to deliver minimum electric power when the natural gas prices are higher than the electricity prices. The fuel cell is allowed to deliver higher electric power when the natural gas prices are lower than the electricity prices. All these indicate that the proposed scheme performs power dispatch optimally regardless of the weather and hot water consumption profiles.

Referring to Figures 12 and 14, these two cases have the same simulation settings except for the solar energy generation profiles used. By comparing these two figures, it can be seen that on the sunny day in Figure 14, the proposed scheme scheduled more electric loads to operate from 10:00 to 15:00 during which solar energy generation is abundant. Moreover, the DFCCHP system sells more electric energy to the power grid in Figure 14 than in Figure 12 because more solar energy is generated from the PV panels. All these are the evidences that the proposed optimization scheme in the HEMS performs efficient energy management by considering all available energy resources and by taking full advantage of electricity price and natural gas price variations.

IX. CONCLUSION

This study proposed a comprehensive electric power and thermal power dispatch scheme for a DFCCHP system that integrates with the residential load scheduling mechanism. Because of the nonlinear characteristics provided by the fuel cell and the use of continuous and binary variables for power dispatch and load scheduling, the proposed scheme was an MINLP formulation with high nonlinearity. The MINLP formulation was solved using a nonlinear branch and bound algorithm. The computation time of this approach is relatively high although the computation time is still very much less than the optimization sampling interval. It is possible to transform the nonlinear functions such as the consuming rate of natural gas or the residual thermal power of the fuel cell into a piecewise linear function for the future work. With delicate arrangement of optimization range, these piecewise linear functions can work in accordance with other linear constraints of the optimization model. The nonlinear optimization problem can be solved efficiently with a regular mixed-integer linear programming formulation in order to save computation time.

As most energy schemes, the proposed scheme performs energy management with a day-ahead solar energy generation profile and a hot water demand profile. Accurate, real-time forecasts of solar energy generation and hot water demand profiles could further enhance the power dispatch accuracy in the proposed scheme in future work.

REFERENCES

[1] S. Ali, I. Khan, S. Jan, and G. Hafeez, "An optimization based power usage scheduling strategy using photovoltaic-battery system for demand-side management in smart grid," *Energies*, vol. 14, no. 8, p. 2229, Apr. 2021.

[2] P. Halder, K. Azad, S. Shah, and E. Sarker, "Prospects and technological advancement of cellulosic bioethanol ecofuel production," in *Advances in Eco-Fuels for a Sustainable Environment*. Sawston, U.K.: Woodhead Publishing, 2019, pp. 211–236.

[3] M. Vohra, J. Manwar, R. Manmode, S. Padgilwar, and S. Patil, "Bioethanol production: Feedstock and current technologies," *J. Environ. Chem. Eng.*, vol. 2, no. 1, pp. 573–584, Mar. 2014.

[4] L. Barelli, G. Bidini, F. Gallorini, and A. Ottaviano, "Dynamic analysis of PEMFC-based CHP systems for domestic application," *Appl. Energy*, vol. 91, no. 1, pp. 13–28, 2012.

[5] F. Calise, M. Dentice d'Accadia, A. Palombo, and L. Vanoli, "Simulation and exergy analysis of a hybrid solid oxide fuel cell (SOFC)–gas turbine system," *Energy*, vol. 31, no. 15, pp. 3278–3299, Dec. 2006.

[6] F. Accurso, M. Gandiglio, M. Santarelli, J. Buunk, T. Hakala, J. Kiviaho, S. Modena, M. Münch, and E. Varkaraki, "Installation of fuel cell-based cogeneration systems in the commercial and retail sector: Assessment in the framework of the COMSOS project," *Energ. Convers. Manage.*, vol. 239, pp. 114202–114222, Jul. 2021.

[7] Z. Zakaria, S. K. Kamarudin, and K. A. A. Wahid, "Fuel cells as an advanced alternative energy source for the residential sector applications in Malaysia," *Int. J. Energy Res.*, vol. 45, no. 4, pp. 5032–5057, Mar. 2021.

[8] Z. Zakaria, S. K. Kamarudin, K. A. A. Wahid, and S. H. A. Hassan, "The progress of fuel cell for Malaysian residential consumption: Energy status and prospects to introduction as a renewable power generation system," *Renew. Sustain. Energy Rev.*, vol. 144, Jul. 2021, Art. no. 110984.

[9] S. You, F. Marra, and C. Træholt, "Integration of fuel cell micro-CHPS on low voltage grid: A Danish case study," in *Proc. Power Energy Eng. Conf.*, Mar. 2012, pp. 1–4.

[10] G. Gigliucci, L. Petruzzi, E. Cerelli, A. Garzisi, and A. La Mendola, "Demonstration of a residential CHP system based on PEM fuel cells," *J. Power Sources*, vol. 131, nos. 1–2, pp. 62–68, 2004.

[11] M. J. Sanjari, H. Karami, and H. B. Gooi, "Micro-generation dispatch in a smart residential multi-carrier energy system considering demand forecast error," *Energy Convers. Manage.*, vol. 120, pp. 90–99, Jul. 2016.

[12] M. Bornapour, R.-A. Hooshmand, A. Khodabakhshian, and M. Parastegari, "Optimal coordinated scheduling of combined heat and power fuel cell, wind, and photovoltaic units in micro grids considering uncertainties," *Energy*, vol. 117, pp. 176–189, Dec. 2016.

[13] M. Houwing, R. R. Negenborn, and B. De Schutter, "Demand response with micro-CHP systems," *Proc. IEEE*, vol. 99, no. 1, pp. 200–213, Jan. 2011.

[14] M. Houwing, R. R. Negenborn, M. D. Ilic, and B. De Schutter, "Model predictive control of fuel cell micro cogeneration systems," in *Proc. Int. Conf. Netw., Sens. Control*, Okayama, Japan, Mar. 2009, pp. 708–713.

[15] H. C. Jo, S. Kim, and S. K. Joo, "Smart heating and air conditioning scheduling method incorporating customer convenience for home energy management system," *IEEE Trans. Consum. Electron.*, vol. 59, no. 2, pp. 316–322, May 2013.

[16] S. Sharma, A. Verma, Y. Xu, and B. K. Panigrahi, "Robustly coordinated bi-level energy management of a multi-energy building under multiple uncertainties," *IEEE Trans. Sustain. Energy*, vol. 12, no. 1, pp. 3–13, Jan. 2021.

[17] A. Anvari-Moghaddam, H. Monsef, and A. Rahimi-Kian, "Optimal smart home energy management considering energy saving and a comfortable lifestyle," *IEEE Trans. Smart Grid*, vol. 6, no. 1, pp. 324–332, Jan. 2015.

[18] F. Barbir and T. Gomez, "Efficiency and economics of proton exchange membrane (PEM) fuel cells," *Int. J. Hydrogen Energy*, vol. 21, no. 10, pp. 891–901, Oct. 1996.

[19] H. A. Abdelsalam, A. K. Srivastava, and A. Eldosouky, "Blockchain-based privacy preserving and energy saving mechanism for electricity prosumers," *IEEE Trans. Sustain. Energy*, vol. 13, no. 1, pp. 302–314, Jan. 2022, doi: 10.1109/TSTE.2021.3109482.

[20] A. U. Rehman, Z. Wadud, R. M. Elavarasan, G. Hafeez, I. Khan, Z. Shafiq, and H. H. Alhelou, "An optimal power usage scheduling in smart grid integrated with renewable energy sources for energy management," *IEEE Access*, vol. 9, pp. 84619–84638, 2021.

[21] E. M. Ahmed, R. Rathinam, S. Dayalan, G. S. Fernandez, Z. M. Ali, S. H. E. Aleem, and A. I. Omar, "A comprehensive analysis of demand response pricing strategies in a smart grid environment using particle swarm optimization and the strawberry optimization algorithm," *Mathematics*, vol. 9, no. 18, pp. 2338–2361, 2021.

[22] M. J. Sanjari, H. Karami, and H. B. Gooi, "Analytical rule-based approach to online optimal control of smart residential energy system," *IEEE Trans. Ind. Informat.*, vol. 13, no. 4, pp. 1586–1597, Aug. 2017.

[23] Y. Huang, J. Zhang, Y. Mo, S. Lu, and J. Ma, "A hybrid optimization approach for residential energy management," *IEEE Access*, vol. 8, pp. 225201–225209, 2020.

[24] Y. Huang, W. Wang, and B. Hou, "A hybrid algorithm for mixed integer nonlinear programming in residential energy management," *J. Cleaner Prod.*, vol. 226, pp. 940–948, Jul. 2019.

[25] M. K. Rafique, S. U. Khan, M. S. U. Zaman, K. K. Mehmood, Z. M. Haider, S. B. A. Bukhari, and C.-H. Kim, "An intelligent hybrid energy management system for a smart house considering bidirectional power flow and various EV charging techniques," *Appl. Sci.*, vol. 9, no. 8, p. 1658, Apr. 2019.

[26] H. Karami, M. J. Sanjari, S. H. Hosseinian, and G. B. Gharehpetian, "An optimal dispatch algorithm for managing residential distributed energy resources," *IEEE Trans. Smart Grid*, vol. 5, no. 5, pp. 2360–2367, Sep. 2014.

[27] W. Violante, C. A. Cañizares, M. A. Trovato, and G. Forte, "An energy management system for isolated microgrids with thermal energy resources," *IEEE Trans. Smart Grid*, vol. 11, no. 4, pp. 2880–2891, Jul. 2020.

[28] B. Borchers and J. E. Mitchell, "An improved branch and bound algorithm for mixed integer nonlinear programs," *Comput. Oper. Res.*, vol. 21, no. 4, pp. 359–367, Apr. 1994.

[29] S. Lee and H. kim, "Fast mixed-integer AC optimal power flow based on the outer approximation method," *J. Electr. Eng. Technol.*, vol. 12, pp. 2187–2195, Nov. 2017.

[30] H.-T. Roh and J.-W. Lee, "Residential demand response scheduling with multiclass appliances in the smart grid," *IEEE Trans. Smart Grid*, vol. 7, no. 1, pp. 94–104, Jan. 2016.

[31] S. He, E. Prempain, and Q. H. Wu, "An improved particle swarm optimizer for mechanical design optimization problems," *Eng. Optim.*, vol. 36, no. 5, pp. 585–605, Oct. 2004.

[32] S. S. Rao and Y. Xiong, "A hybrid genetic algorithm for mixed-discrete design optimization," *J. Mech. Des.*, vol. 127, no. 6, pp. 100–112, Nov. 2005.

[33] J. Lampinen and I. Zelinka, "Mixed integer discrete continuous optimization by differential evolution. Part 1: The optimization method," in *Proc. 5th Int. Mender Conf. Soft Comput.*, 1999, pp. 71–76.

[34] T. Niknam, M. Bornapour, A. Ostadi, and A. Gheisari, "Optimal planning of molten carbonate fuel cell power plants at distribution networks considering combined heat, power and hydrogen production," *J. Power Sources*, vol. 239, pp. 513–526, Oct. 2013.

[35] C. Ou, C. Xie, J. Xu, and F. Liu, "Time-of-use price decision model of natural gas based on simulation and grey relationships," in *Proc. IEEE Int. Conf. Inf. Manage., Innov. Manage. Ind. Eng. (ICIII)*, Nov. 2010, pp. 176–179.

[36] C. Gong, K. Tang, K. Zhu, and A. Hailu, "An optimal time-of-use pricing for urban gas: A study with a multi-agent evolutionary game-theoretic perspective," *Appl. Energy*, vol. 163, pp. 283–294, Feb. 2016.

[37] M. Tasdighi, H. Ghasemi, and A. Rahimi-Kian, "Residential microgrid scheduling based on smart meters data and temperature dependent thermal load modeling," *IEEE Trans. Smart Grid*, vol. 5, no. 1, pp. 349–357, Jan. 2014.

[38] A. Ouammi, "Optimal power scheduling for a cooperative network of smart residential buildings," *IEEE Trans. Sustain. Energy*, vol. 7, no. 3, pp. 1317–1326, Jul. 2016.

LEEHTER YAO (Senior Member, IEEE) received the Diploma degree in electrical engineering from the National Taipei Institute of Technology, Taipei, Taiwan, in 1982, the M.S. degree in electrical engineering from the University of Missouri, Rolla, in 1987, and the Ph.D. degree in electrical engineering from the University of Wisconsin–Madison, in 1992. Since 1992, he has been with the Department of Electrical Engineering, National Taipei University of Technology, where he is currently a Chair Professor. He has held over 30 patents mostly in the areas of power system monitoring and control, and industrial applications of computational intelligence. His current research interests include intelligent control, demand response, and computational intelligence. He was a recipient of the Distinguished Electrical Engineering Professor Award from the Chinese Society of Electrical Engineering, in 2011. Since 2015, he has been the Academician of the Russia International Academy of Engineering.

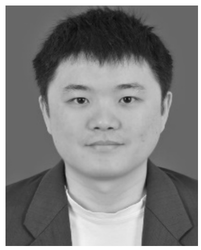

J. C. TEO received the B.S. and Ph.D. degrees in electrical and electronic engineering from UCSI University, Kuala Lumpur, Malaysia, in 2014 and 2020, respectively.

He is currently a Postdoctoral Researcher with the Department of Electrical Engineering, National Taipei University of Technology, Taipei, Taiwan. His current research interests include home energy management systems and energy management system of fuel cell.